Pediatr Radiol (2000) 30: 289–298

Accuracy of MR imaging for detecting epiphyseal extension of osteosarcoma

Fredric A. Hoffer
Alexander Y. Nikanorov
Wilburn E. Reddick
Sara M. Bodner
Xiaoping Xiong
Dana Jones-Wallace
Suzanne A. Gronemeyer
Bhaskar N. Rao
William M. Kauffman
Tal Laor

Received: 20 August 1999
Accepted: 13 January 2000

F. A. Hoffer (✉) · A. Y. Nikanorov · W. E. Reddick · S. A. Gronemeyer · W. M. Kauffman
Department of Diagnostic Imaging, St. Jude Children's Research Hospital, 322 N. Lauderdale St., Memphis TN 38105-2794, USA

S. M. Bodner
Department of Pathology, St. Jude Children's Research Hospital, Memphis TN, USA

X. Xiong · D. Jones-Wallace
Department of Biostatistics, St. Jude Children's Research Hospital, Memphis, TN, USA

B. N. Rao
Department of Surgery, St. Jude Children's Research Hospital, Memphis, TN, USA

T. Laor
Department of Radiology, Children's Hospital Medical Center, Cincinnati, OH, USA

Abstract *Background.* Too few patients are receiving epiphyseal-sparing limb salvage procedures for osteosarcoma.
Objective. To determine how magnetic resonance (MR) imaging can best predict the epiphyseal extension of osteosarcoma.
Materials and methods. Forty children underwent complete pretreatment static and dynamic contrast-enhanced MR imaging (DEMRI). Static MR images [T1-weighted and short tau inversion recovery (STIR)] of the epiphyses were read in three ways: (1) for suspicion of any abnormality (tumor or edema), (2) for suspicion of tumor, excluding suspected edema, and (3) validating the second method by using a scale to rate the likelihood of tumor. Presentation imaging was compared to histopathologic findings after chemotherapy and resection. The receiver operating characteristic (ROC) method was used to analyze the scaled ratings of static MR and DEMRI values.
Results. At delayed resection, 20 of 40 children with osteosarcoma had confirmed epiphyseal tumor; however, 32 epiphyses were abnormal on STIR and 28 abnormal on T1. Differentiating suspected tumor from edema increased the accuracy to an A_z (area under the ROC curve) of 0.94 for both T1-weighted and STIR static sequences. T1-weighted MR had better specificity and STIR better sensitivity at any given rating. DEMRI was slightly less accurate (Az = 0.90).
Conclusion. Static MR imaging most accurately detected epiphyseal extension of osteosarcoma when readers distinguished suspected tumor from edematous or normal tissue.

Introduction

When performing limb-salvage procedures for pediatric patients with osteosarcoma, surgeons in the past have performed wide resections using osteoarticular allografts or metallic prostheses. With better chemotherapy and imaging regimens, the requirement for broad (5 cm) surgical margins has decreased to 1–2 cm, and the surgeon may prefer to leave the epiphysis intact with a segmental (intercalary) resection when possible. Sparing the physis may be significant to the very young in whom growth is essential. In addition, sparing the epiphysis tends to preserve the natural joint and achieve a better functional outcome than osteoarticular grafts or metallic prostheses [1].

The cartilaginous physis in children should serve as a natural barrier to the spread of osteosarcoma from metaphysis to epiphysis, but this barrier is breached 70 %

of the time by osteosarcoma according to one study [2]. To date, no optimal method has been established for the presurgical identification of epiphyseal tumor extension. Prior reports suggest that T1-weighted MR imaging detects epiphyseal extension of osteosarcoma with 100% sensitivity and specificity [2, 3], but the cited studies were small and did not always include pathologic confirmation. Another report concluded that short tau inversion recovery (STIR) imaging overestimates the extent of medullary tumor involvement [4]. However, that study identified tumor involvement by findings that differed from those of the contralateral side, and results may thus have been confounded by peritumoral edema. Dynamic contrast-enhanced MR imaging (DEMRI) has been successfully used to assess tumor viability or necrosis [5–8] and the diaphyseal extent of osteosarcoma [9], but its accuracy in detecting epiphyseal extension is not known. MR assessment of tumor extent becomes even more difficult after chemotherapy accompanied by granulocyte colony-stimulating factor (G-CSF), which may convert fatty epiphyseal marrow to hematopoietic marrow [10, 11].

To determine whether MR studies at presentation can predict the finding of epiphyseal extension of osteosarcoma at delayed resection, we compared the accuracy of two routine pre-contrast static MR sequences and experimental dynamic contrast-enhanced MR findings at presentation, as determined by the post-surgical histopathologic studies. To determine whether DEMRI could distinguish among malignant, edematous, and normal epiphyses, we compared abnormal MR signals in the malignant and nonmalignant portions of the epiphysis.

Materials and methods

Patient selection

Between January 1992 and July 1997, 72 patients with osteosarcoma were prospectively enrolled on an institutional treatment protocol that included MR imaging. Of these, 40 patients were retrospectively selected who had (1) DEMRI, T1-weighted, and STIR MR imaging at presentation, (2) MR imaging at 1.5-T field strength, and (3) a tumor in a long bone. There were 22 males and 18 females, aged 6 to 20 years (median, 13 years). Tumor sites included femur (28), tibia (7), humerus (4), and fibula (1). The three tumors that appeared to be confined to the diaphysis on MR imaging were not excluded from the analysis due to potential statistical bias on the results.

Treatment protocol

Before resection, all patients received three cycles of intravenous ifosfamide (2.65 g/m^2 per day × 3 days) and carboplatin (560 mg/m^2), which were given at 3-week intervals over 9 weeks [12]. All received G-CSF. All but two patients had en bloc resection, including the nearest epiphysis. Two patients had an epiphyseal-sparing intercalary limb salvage procedure. Most underwent limb salvage with metallic prostesis, and a few underwent amputation.

Imaging

Identical DEMRI and routine static MR imaging studies were performed at presentation and before resection. Only the presentation MR imaging was analyzed because surgical decisions are usually made on the basis of the initial imaging. The preresection MR images were not retrospectively analyzed for the purposes of this paper, except in cases where the resection pathology was discordant with the presentation MR imaging.

Static MR imaging comprised longitudinal T1-weighted (SE 600–800/15) and STIR 3500/18 TI: 140) and transverse T2-weighted and contrast-enhanced T1-weighted images. For DEMRI, a 1.5 T SP63 Magnetom imager (Siemens Medical Systems; Iselin, N.I.) was used, with the standard quadrature body coil as transmitter and receiver. After selection of the longitudinal (usually coronal) section that best showed the tumor, 30 sequential fast low-angle shot (FLASH) images (TR/TE = 23/10 ms, 40° flip angle, 256 phase incodings, 10-mm slice thickness, 40- to 50-cm field of view, 2 acquisitions) were acquired over a 7-min period before, during, and after a bolus hand injection of 0.1 mmol/kg of gadolinium (Nycomed Inc., Princeton, N.I.), as described previously [13, 14]. Sagittal images were preferred for humeral imaging. The opposite epiphysis was included on lower extremity imaging, but not on upper-extremity imaging.

Quantitative image analysis (DEMRI)

Dynamic vector magnitude

Dynamic vector magnitude (DVM) is a DEMRI parameter that expresses the rate and quantity of contrast medium accumulation in the tumor and is a measure of osteosarcoma viability and necrosis [13, 14]. It was included in this analysis as a potential method of detecting epiphyseal extension of osteosarcoma.

$$\mathrm{DVM} = \sqrt{(\mathrm{ME}/50)^2 + (\mathrm{ICAR})^2}$$

ME is the maximum enhancement as calculated by the difference between the maximum and minimum value in the signal intensity curve. ICAR is the initial contrast accumulation rate that was calculated as the maximum value of the first derivative (rate in SI/s) that occurred in the interval between bolus arrival and 120 s after bolus arrival. An analysis of the distribution of DVM values in a radiologist-selected region of interest (ROI) yielded the mean DVM (μ_{DVM}).

Pharmacokinetic modeling

Because MR contrast medium does not cross cell membranes, it is present only in plasma and extracellular fluid (ECF). Hence, a conventional two-compartment pharmacokinetic model comprising plasma volume and ECF volume was used to analyze contrast distribution in each voxel of the DEMRI images [15–17]. The modeled rate of contrast exchange between the plasma and the tumor ECF (designated k_{21}) was used as the measure of regional access. R is a parameter that combines the tissue- and frequency-dependent relaxivity (β), the fractional extracellular volume (f_{ex}), and the zero-order infusion rate constant (k_{in}).

The contrast agent was infused at a constant rate over approximately 5 s. To simplify the model of signal intensity in the presence of contrast, we assumed a constant elimination rate of 0.06 min^{-1} during the DEMRI examination (resulting in plasma concentrations approximating the empirically determined biexponential

elimination rates reported by Weinmann et al. [18]) and a linear relationship between the total tissue concentration and the ECF concentration, in accord with the Bloembergen equation [19, 20]. We also assumed a constant T1 relaxation time of 700 ms in the absence of contrast. The pharmacokinetic model of regional MR contrast access was then combined with the signal intensity equation for the FLASH imaging sequence to complete the analysis [21, 22]. Mean values of the regional access parameter k_{21} and the combination parameter *R* in the identified ROI were determined for each patient at each examination point.

Interpretation of imaging

Static MR readings

One observer, who was blinded to the pathology findings, categorized epiphyseal involvement by reading the static MR images. T1 and STIR images for each case were separately rated as either 1 or 0 in two categories: (a) suspected involvement of any type (tumor, edema, or both) and (b) suspected tumor involvement. Thus, each case had four ratings. The categories and criteria were

a. Suspected involvement of any type (edema, tumor, or both)
1: Involvement, as determined by a signal unlike that of the contralateral epiphysis
0: No involvement of any type
b. Suspected tumor involvement
1: Tumor involvement (as determined by a signal that was as dark as neighboring tumor on T1, or as bright as tumor on STIR, or that altered the normal architecture of the physis or epiphysis on MR)
0: No tumor involvement (suspected) edema was identified by an intermediate signal on T1 or STIR in which the physis and epiphysis had normal architecture)

In addition, one observer determined if the physis was open based on a bright signal in the physis on the STIR image choosing the closest physis to the tumor or the contralateral physis when the physis was destroyed. Also, he determined if the tumor margin involved the physis. The tumor margin was deemed separated from the physis when normal architecture and intermediate or normal bright signal in the metaphysis was present on every T1-weighted image next to the physis.

Scaled Static MR Rating

Three radiologists who were blinded to the pathology reports (including the one observer who performed the unscaled readings) independently examined the static T1-weighted and STIR images of each patient (Figs. 1–5). For both T1 and STIR, each reader rated the epiphysis on a 5-point scale: 0: definitely not tumor; 1: probably not tumor; 2: indeterminate tumor or other abnormality; 3: probably tumor; 4: definitely tumor. The readers were instructed to rate an intermediate signal on T1 or STIR in which physis and epiphysis had normal architecture as 1 (probably not tumor). The resulting multireader, multicase rating data were subjected to a receiver operating characteristic (ROC) analysis of variance to identify any difference in the areas under the T1-weighted and STIR ROC curves (Az) and to identify any differences among the ratings of the three readers. The LABMRMC software [23] was used for the analysis.

DEMRI

For the analyses of DEMRI, values of DVM, k_{21}, and *R* were determined for: (1) the whole epiphysis; (2) the adjusted whole epiphysis (DEMRI value of affected whole epiphysis – DEMRI value of contralateral normal whole epiphysis); (3) the region of interest (ROI) identified by static MR in the affected epiphysis (order of preference: ROI from suspected tumor, suspected edema, or from the whole epiphysis for those showing no abnormality).

Normal DVM values were missing for six patients and normal k_{21} or *R* values were missing for six patients. These patients were excluded from analyses that used adjusted values. We used the CORROC program [24] to derive the maximum likelihood estimation of the area under the ROC curves (Az) for DVM, k_{21}, and *R* for the whole epiphysis, the whole epiphysis adjusted by contralateral side, and the region of interest (ROI) identified by static MR.

Analysis of imaging interpretation

Resection and histopathologic studies were performed 9 weeks after the initial MR evaluation. Tumor extension into the physis and epiphysis was mapped on coronal sections of excised bone. Absence or presence of the destruction of the physis was noted. The epiphyseal tumor extension was determined by visualizing viable tumor or pale osteoid representing prior neoplastic bone production (Fig. 4 A). Epiphyseal areas that had no tumor involvement but had abnormal MR signal were also investigated by close pathologic review. Determination of epiphyseal extension of tumor in the two patients that did not have the epiphysis resected was based on histopathology of the metaphyseal margins at en bloc resection and the follow-up radiography 2–4 years later.

We used the exact Wilcoxon rank sums test to compare the adjusted DEMRI values from the whole epiphyses that were proved to have tumor with those from epiphyses that had abnormal static MR appearance but were proved to have no tumor. We wished to determine how significantly the affected side in the tumor group and in the abnormal non-tumor group differed from the opposite normal epiphysis. This was done by using the Wilcoxon signed rank test to determine if adjusted DEMRI values (whole affected epiphysis minus opposite normal epiphysis) in the epiphyses under study differed significantly from zero.

Results

Epiphyseal extension of tumor

Twenty of the 40 patients had epiphyseal extension of tumor, as documented by histopathologic studies of bone removed by en block resection (Figs. 1–3). The two patients that had epiphyseal sparing intercalary limb salvage procedures had no tumor at resection margins and no radiographic evidence of tumor recurrence 2–4 years later. All four proximal humeral osteosarcomas had extended into the epiphysis. Seven of 18 females (39 %) and 13 of 22 males (59 %) had epiphyseal extension of tumor.

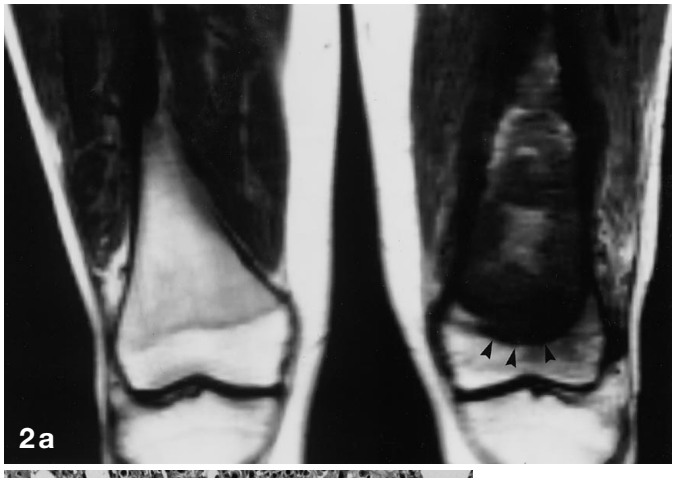

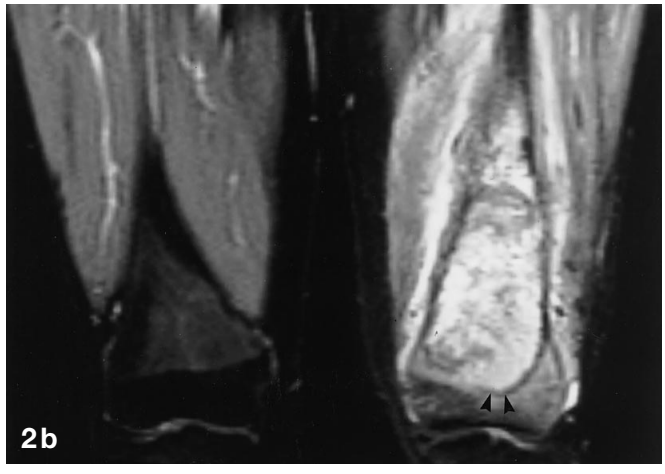

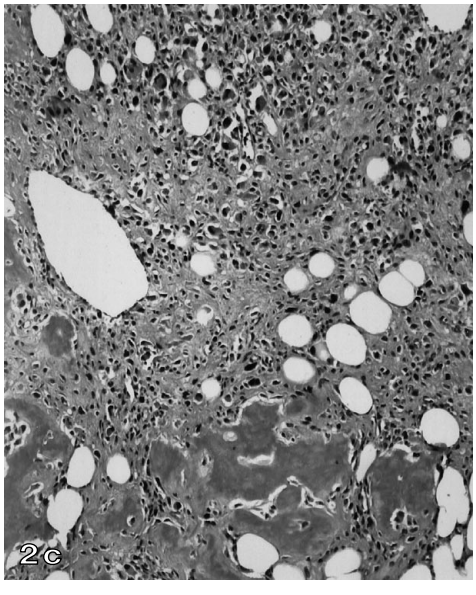

Fig. 1 a, b Local physis invasion. **a** Osteosarcoma extended locally through the right distal femoral open cartilaginous physis in this 11-year-old boy, as demonstrated by T1-weighted MR imaging (SE: 600/15) at presentation. The small dark area *(arrowheads)* was tumor, but the intermediate signal in the remainder of the epiphysis was not. The adjusted whole-epiphysis dynamic vector magnitude (DVM) was 0.88, a level that was 90 % sensitive and 78 % specific for tumor. **b** The physis *(curved arrow)* was locally destroyed by tumor *(arrowheads),* as demonstrated by histopathology (H & E, × 2) at resection

Fig. 2 a–c Aggressive tumor. **a** This 17-year-old male had initial T1-weighted MR imaging (SE: 600/15) that showed dark signal, thought to be tumor *(arrowheads),* extending into the left distal femoral epiphysis. **b** Initial STIR sequence (FSE/IR: 4500/18 eff; 140 tau) also demonstrated bright signal thought to be tumor *(arrowheads).* The adjusted whole-epiphysis DVM was markedly elevated at 3.2, a level that had well over 95 % specificity for tumor. This tumor had grown further into the epiphysis on the 9-week MR, despite chemotherapy. **c** The histopathology (H & E, × 10) at resection demonstrated highly malignant, pleomorphic, and viable tumor

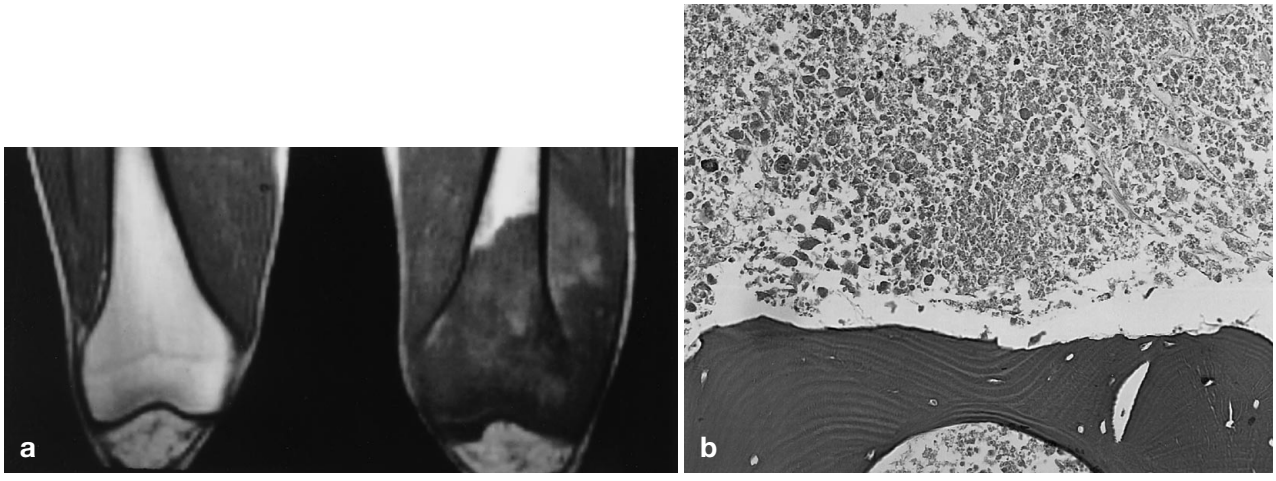

Fig. 3 a, b Necrotic tumor. This 19-year-old male had T1-weighted MR imaging (SE: 600/15) at presentation that was interpreted as definite tumor extension into the epiphysis of the left distal femur on. The adjusted whole-epiphyseal DVM was 1.07, a level that was 80% sensitive and 84% specific for tumor, but was between the 1.95 median value for tumor and the 0.69 median value for edema. This relatively low value may represent necrosis. **b** The epiphysis (H & E, ×20) consisted mostly of necrotic tumor at resection 9 weeks later

Physeal relationship to tumor

Of the 20 patients that had epiphyseal extension of tumor by histopathological study, 13 had an open physis by STIR MR and 7 were closed. Of the 20 patients that did not have epiphyseal extension of tumor, 18 had an open physis and 2 were closed.

By T1-weighted imaging, the suspected tumor margin was separate from the physis in only 8 cases. None of the eight cases had tumor in the epiphysis. The separation of the suspected tumor margin from the physis on T1 weighted MR in these 8 cases was at a median of 1.75 cm (range 0.2–9.0 cm). Five of the tumors extended to or arose in the metaphysis. Only three of the tumors (separation 7.5, 7.5, 9.0 cm) were considered diaphyseal.

By T1-weighted imaging, the suspected tumor margin was contiguous with or overran the physis in 32 of 40 patients. Only 20 of these 32 patients had epiphyseal spread of osteosarcoma. Twelve of the 32 did not have epiphyseal spread of osteosarcoma.

Static MR imaging of the epiphysis

Both T1-weighted and STIR imaging had 100% sensitivity for detecting suspected tumor or edema; however, they had poor tumor specificity (T1, 60%; STIR, 40%). Eight patients were misclassified as having epiphyseal tumor extension on the basis of T1, and 12 patients were misclassified on the basis of STIR, yielding false-positive rates of 40% and 60%, respectively.

When only suspected tumor was considered, STIR had better tumor sensitivity (95%) than did T1 (90%), and T1 had better tumor specificity (90%) than did STIR (70%). Only four patients were misclassified (two false-positives and two false-negatives) on the basis of T1 (Fig. 4). In comparison, seven patients were misclassified (one false-negative and six false-positives) on the basis of STIR (Fig. 5). Therefore, of the static imaging, T1 images rated only for the presence or absence of suspected tumor were more accurate than STIR images.

Scaled rating of static MR imaging of epiphysis

We wished to determine whether the ratings of static MR images were consistent among the three observers and which modality was a better predictor of tumor invasion of the epiphysis, as further validated by the scaled ratings. The true positive fraction (TPF) and false-positive fraction (FPF) for each of the five ratings were estimated for both T1-weighted and STIR images. The TPF and FPF were used to compare potential rating thresholds for distinguishing tumor from non-tumor. ROC curves (Fig. 6) were generated for these scaled ratings. The analysis of variance for the ROC curves showed no significant difference between the diagnostic accuracy of T1 and that of STIR ($P = 0.94$) and no significant interreader disagreement ($P = 0.38$). The mean area under the ROC curves (A_z) of the three readers was 0.9355 (95% C.I., 0.85–1.00) for T1 and 0.9336 (95% C.I., 0.87–0.99) for STIR. Table 1 shows the relationship between the estimated TPF and FPF for T1 and STIR ratings from one observer (FAH). This relationship is represented by the ROC curve shown in Fig. 6.

Fig. 4a–c Epiphyseal tumor retraction. **a** This 11-year-old boy underwent T1-weighted MR imaging (SE: 600/15) of the distal left femur at presentation that showed probable tumor invasion *(arrowheads)* through the open physis *(curved arrow)*. The adjusted whole-epiphyseal DVM was 1.63, a level that was 93% specific for tumor. **b** At week 9, on T1-weighted MR imaging, the femur measured 1 cm longer and had an intermediate signal in the epiphysis *(arrowheads)*. **c** Pathologic examination (H & E, × 2) showed that the growth plate *(white arrow)* was destroyed, but the epiphysis contained only a local focus of hematopoietic marrow. Tumor, as shown by pale tumor ossification *(arrowheads)*, was found only in the metaphysis. Retraction of epiphyseal tumor or growth of the metaphysis in the 9 weeks between imaging and resection caused this "false-positive" result

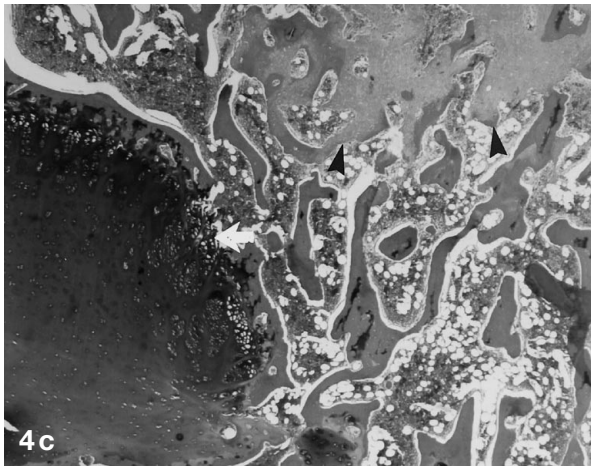

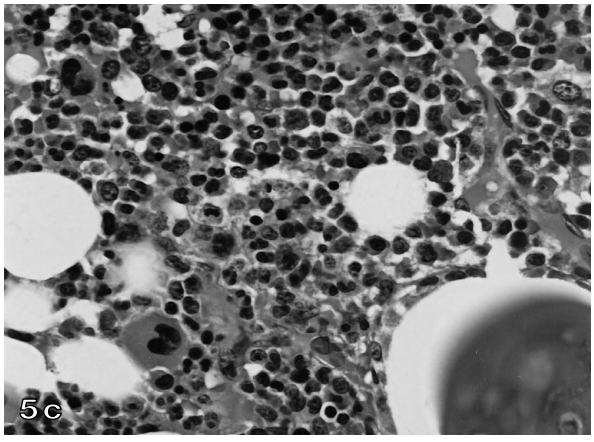

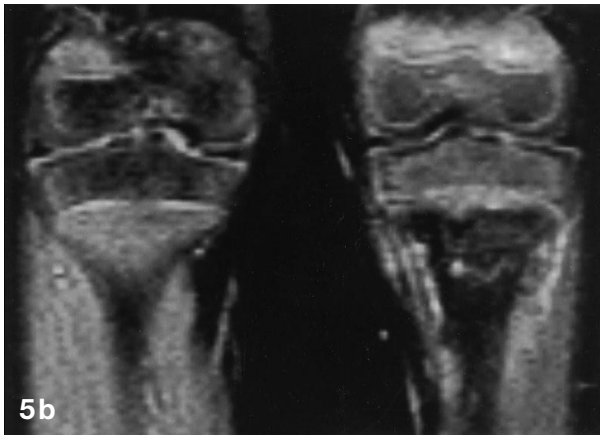

Fig. 5a–c Edema and hematopoiesis. This 7-year-old boy had initial STIR MR imaging (FSE/IR: 4500/18 eff; 140 tau) that showed a bright signal in the affected left proximal tibial epiphysis *(open arrows)*. The normal architecture of the physis and epiphysis was intact. The mean ROC rating was 2 or "indeterminate" for edema versus tumor. T1-weighted MR had an intermediate signal with a mean ROC rating of 1, "probably not tumor." The adjusted DVM was 1.81, a value that was 94% specific for tumor. The adjusted R was 0.13×10^{-3}, indicating edema. **b** At week 9, all epiphyses produced an intermediate signal on STIR MR imaging. **c** Histopathology (H & E, × 40) demonstrated hematopoetic marrow with no tumor or edema in the epiphysis. The initial bright signal on STIR may have reflected pretreatment edema and hematopoesis caused by regional angiogenesis. The intermediate signal of all the epiphyses at 9 weeks probably reflected conversion of yellow marrow to red marrow by granulocyte colony-stimulating factor

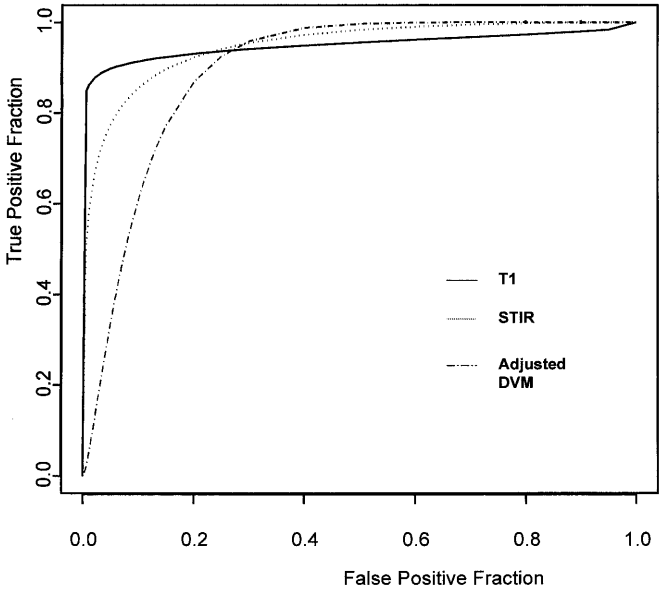

Fig. 6 ROC analysis. Receiver operating curves representing one observer's (F. A. H.) reading of static T1-weighted and STIR images from all 40 patients and adjusted whole-ephiphyseal DVM from the available 34 patients. The Y axis is the true positive fraction (TPF). A TPF of 1.0 reflects 100 % sensitivity. The X axis is the false-positive fraction (FPF). A FPF of 0.0 reflects 100 % specificity. The ROC demonstrates that T1 in general is most specific, adjusted DVM is most sensitive, and STIR is intermediate. However, sensitivity and specificity of each MR parameter vary with the threshold rating or value chosen. The area under the curve (Az), a measure of accuracy, was 0.94 for T1 and STIR and 0.90 for adjusted DVM. The perfect curve (Az = 1.0) would make a 90° angle in the extreme left upper corner

Table 1 Estimated true positive and false-positive fractions[a] in static and dynamic contrast-enhanced MR imaging of epiphyses

T1	Rating	TPF	FPF
	0	0.96	0.49
	1	0.93	0.23
	2	0.91	0.12
	3	0.80	0.007
	4	0.47	0.0000007
STIR	Rating	TPF	FPF
	0	0.999	0.87
	1	0.98	0.47
	2	0.93	0.21
	3	0.76	0.05
	4	0.25	0.0006
DEMRI	Adjusted DVM Value	TPF	FPF
	0.33	0.99	0.41
	0.47	0.98	0.36
	0.56	0.97	0.33
	0.66	0.96	0.29
	0.73	0.94	0.27
	0.77	0.93	0.25
	0.84	0.91	0.23
	0.87	0.90	0.22
	0.95	0.87	0.20
	1.06	0.80	0.16
	1.54	0.54	0.08
	1.69	0.44	0.07
	1.78	0.39	0.06
	1.86	0.33	0.05

[a] The TPF (true positive fraction) and FPF (false-positive fraction) correspond to a sliding scale, assuming that the given rating (or value) and those higher indicate tumor

Dynamic contrast-enhanced MR imaging of epiphysis

By using ROC analysis for correlated measurements, we obtained the estimated areas under the ROC curve for the whole-epiphyseal DEMRI values. The DVM (Az = 0.82, SE = 0.067) was the most accurate DEMRI parameter to distinguish tumor from non-tumor, followed by R (Az = 0.79, SE = 0.071) and k_{21} (Az = 0.57, SE = 0.090).

Because the DEMRI values of the normal (contralateral) epiphysis in the confirmed tumor group were smaller than those in the confirmed non-tumor group, we adjusted the DEMRI values by subtracting the value of the normal (contralateral) epiphysis from that of the affected epiphysis. Normal DVM values were missing for 6 of the 40 patients (4 in the tumor group and 2 in the non-tumor group), and normal k_{21} or R values were missing for 6 patients (4 in the tumor group and 2 in the non-tumor group). These patients were excluded from analyses that used adjusted values. The estimated area under the ROC curve increased for all three adjusted DEMRI values. Adjusted DVM of the whole epiphysis remained the most accurate DEMRI value (Az = 0.90, SE = 0.055), followed by adjusted R (Az = 0.84, SE = 0.066) and adjusted k_{21} (Az = 0.74, SE = 0.084). The ROC curves of the scaled T1 and STIR readings from one observer were plotted against the ROC curve of adjusted DVM (Fig. 6).

The ROC curve can be used to provide inferential information for tumor diagnosis on the basis of calculation of the TPF and FPF from a patient's DEMRI values. Table 1 lists the TPF and FPF for several values of adjusted DVM (affected whole epiphysis minus normal contralateral side) that were plotted in the ROC curve shown in Fig. 6.

The DVM values based on a preferential ROI had an accuracy (Az = 0.87, SE = 0.06) between those of the unadjusted whole epiphysis (Az = 0.82, SE = 0.067) and the adjusted whole epiphysis (Az = 0.90, SE = 0.06).

To investigate whether DEMRI can differentiate among tumor, edema, and normal tissue when suspected tumor or edema are identified by static MR imaging, we

Table 2 DEMRI analysis of epiphyses that appeared abnormal on static MR (*DEMRI* dynamic contrast-enhanced MR imaging; MR: magnetic resonance, *DVM* dynamic vector magnitude; a DEMRI measure of viability, k_{21} a DEMRI measure of regional access, *R* a DEMRI measure of extracellular fluid)

Adjusted* DEMRI parameter	Status of affected epiphysis	Number of patients	Median value	DEMRI of affected side vs. normal** (*P*-value)***	DEMRI of tumor vs. non-tumor (*P*-value)***
DVM	Tumor	16	1.95	0.0001	
	Not tumor	10	0.69	0.010	
					0.005
k_{21}	Tumor	16	0.015	0.001	
	Not tumor	11	0.0014	0.83	
					0.011
R	Tumor	16	0.40×10^{-3}	0.0001	0.091
	Not tumor	11	0.178×10^{-3}	0.003	

* Value of whole affected epiphysis – value of contralateral normal epiphysis

** The adjusted DEMRI parameter of a normal epiphysis should be 0

*** Statistically different if *P* value = < 0.05

compared the adjusted DEMRI values of the confirmed tumor group ($n = 20$) to those of the confirmed non-tumor group ($n = 12$; Table 2). Our analysis showed that DVM, k_{21}, and *R* can distinguish tumor from normal tissue ($P = 0.0001$, 0.001, and 0.0001, respectively), and that *R* and DVM can distinguish suspected edema from normal tissue ($P = 0.003$ and 0.010, respectively). The median adjusted DVM and k_{21} values differed significantly between the tumor group and the non-tumor group ($P = 0.005$ and $P = 0.011$, respectively).

Dicussion

Rationale for precise tumor margin detection

We have been in a unique position of performing metallic prostheses for most of our limb salvages, allowing us to study the epiphyseal involvement with MR at presentation and documenting the involvement with histopathology from the resected epiphysis. As smaller 1–2 cm margins are required in part due to accurate MR diagnosis of margin position [25–27], intercalary limb salvage and the osteoarticular graft are more feasible alternatives for limb salvage, depending on the degree of epiphyseal involvement. Hopefully, this information will allow more epiphyseal-sparing limb salvage in the future.

Theoretically, if the tumor margin is over 1 cm from the physis, then physeal-sparing intercalary limb salvage can be performed. From our small series, none of our 8 patients who had a margin of normal metaphysis between the tumor and physis by T1-weighted imaging had physeal or epiphyseal tumor. Physeal-sparing surgery allows adequate growth potential in those patients with an open growth plate. This is especially important for the younger patient who has many years of growth potential remaining. No growth on the side of the tumor may cause a relatively short limb and leg length discrepancy, requiring surgical closure of the opposite physis or osteotomy of the opposite extremity.

If the tumor margin is between 0 and 1 cm of the physis but not beyond, then the physis may need resection; but most of the epiphysis can be spared. Epiphyseal-sparing surgery may allow a more functional joint than the osteoarticular graft or metallic prosthesis.

How one determines that the epiphysis is tumor free by the initial MR is the subject of the following discussion.

Accuracy of MR imaging for detection of epiphyseal osteosarcoma

In an all-or-none approach, in which any abnormal epiphyseal marrow is considered tumor, static MR imaging is 100 % sensitive but only 40–60 % specific for tumor. As previously reported [4], this approach does not distinguish tumor from other abnormalities. This method would allow only 20 % (8 of 40) of our patients to be offered an intercalary graft; an additional 30 % (12 of 40) would have been denied this procedure despite the absence of epiphyseal tumor extension.

The accuracy of tumor diagnosis improves when suspected tumor is distinguished from suspected edema (ROC Az = 0.94). Epiphyseal extension of osteosarcoma is indicated by a dark signal on T1 and a bright signal on STIR or by disturbance of the normal architecture of the physis or epiphysis (Figs. 1–4). Peritumoral effects (possible edema, hematopoietic marrow, or angiogenesis) usually show an intermediate signal on T1 or

STIR imaging, have indistinct margins, and do not disturb the physeal or epiphyseal architecture (Fig. 5). The ROC analysis we performed (Fig. 6; Table 1) may allow a surgeon to determine the relative risk of positive surgical margins. Although observations of T1 and STIR MR sequences were equally accurate, STIR was more sensitive overall and T1 was more specific.

Because static imaging interpretation is subjective, we investigated DEMRI as an objective method for detecting epiphyseal extension of osteosarcoma (Table 1). In individual cases, DEMRI may add useful information to the static MR assessment of epiphyses (Figs. 1–5). DVM, a measure of tumor viability, was the most useful of the DEMRI parameters. In our opinion, the whole-epiphysis DVM value offers the most objective method for determining tumor spread. DVM analysis of a chosen region of interest within the epiphysis yields more accurate results, but is less objective. The adjusted DVM was the most accurate and objective DEMRI measure of tumor spread, but was less accurate (Az = 0.90, Fig. 6) than static imaging (Az = 0.94). For clinical decision making, static MR imaging is most accurate and practical.

There are inherent problems in using only the presurgical MR imaging to determine epiphyseal spread of osteosarcoma. G-CSF used during neoadjuvant chemotherapy causes yellow to red marrow conversion [10, 11], making the tumor margin less certain (Fig. 5). In addition, surgical options are often determined on the pretreatment MR imaging, It is still important to perform the presurgical MR for the relatively rare case of tumor progression during neoadjuvant chemotherapy (Fig. 2) or tumor retraction into the metaphysis with bone growth (Fig. 4).

The nature of non-tumor epiphyseal abnormality at presentation

An intermediate signal on initial static T1 and STIR MR imaging indicated edema, as determined by analysis of the DEMRI parameters. The *R* parameter was able to detect a greater-than-normal extracellular fractional fluid volume in the epiphyseal marrow adjacent to metaphyseal tumor ($P = 0.003$; Table 2). Tumor in the epiphysis also had a greater-than-normal extracellular fractional volume ($P = 0.0001$), but it was not significantly greater than that of the abnormal non-tumor epiphysis ($P = 0.09$). Interruption or compression of the lymphatic flow by neighboring tumor could explain this edema. Venous compression by proximal tumor or increased capillary blood pressure caused by arterial vasodilatation may also cause elevated interstitial fluid pressure and edema.

The DVM, which provides a combined measure of the flow rate and quantity of contrast medium that enters the epiphysis, was significantly greater in tumor than in non-tumor abnormal areas and was smallest in the contralateral normal epiphysis (Table 2). These findings suggest that the non-tumor containing epiphysis that was abnormal on static MR imaging had greater-than-normal perfusion.

k_{21}, a regional access constant that measures the rate at which the contrast medium crosses from the vascular to the interstitial space, is dependent on both perfusion and vessel permeability. Elevated k_{21} in the tumor-involved epiphyses probably reflected tumor angiogenesis with greater microvascular density and greater vessel permeability. However, k_{21} was not elevated in edematous or normal epiphyses whose vessels were not abnormally permeable.

Could a regional angiogenesis factor cause the abnormal imaging findings in the epiphysis next to a metaphyseal tumor? When the physis is open, it is composed of cartilage, a known inhibitor of angiogenesis. Tumor angiogenesis may only occur within millimeters of a tumor. A regional angiogenesis factor that stimulated the growth of normal vessels in the epiphysis could convert epiphyseal fatty marrow to hematopoietic marrow. Vessels in the edematous epiphyses did not leak, unlike tumor-associated vessels.

The suspected edema in the adjacent epiphyses that was noted on initial static MR was correlated with hematopoiesis at the time of post-treatment pathologic examination. It may be difficult to detect edema on pathologic examination. The normal epiphysis has a bright signal on T1-weighted images, reflecting the predominance of fatty marrow. We suspect that the intermediate signal on the initial static MR reflected both edema and conversion of fatty marrow to hematopoietic marrow. The same hypothetical factors that caused the edema may have caused the pretreatment hematopoesis and marrow conversion.

Conclusion

Static MR imaging accurately detected the epiphyseal extension of osteosarcoma when the observer distinguished tumor from non-tumoral abnormality. DEMRI, a more objective method, was not as accurate as static T1 and STIR imaging. However, DEMRI gave us insight into the nature of the abnormal non-tumor signal in the tumor-adjacent epiphyses on initial MR studies, suggesting edematous and hematopoetic marrow.

Acknowledgements We wish to thank Jennifer Kaufman for gathering the images, Sharon Naron for editing the manuscript, Charles Metz, Department of Radiology, University of Chicago, for developing the ROC analysis software, Dr. Michael Neel for his suggestions, and Dr. Barry Fletcher for his support. This work was supported in part by Cancer Center Support (CORE) grant CA21765 from the National Cancer Institute and by the American Lebanese Syrian Associated Charities (ALSAC).

References

1. Mankin HJ, Gebhardt MC, Jennings LC, et al (1996) Long-term results of allograft replacement in the management of bone tumors. Clin Orthop 324: 86–97
2. Panuel M, Gentet JC, Scheiner C, et al (1993) Physeal and epiphyseal extent of primary malignant bone tumors in childhood. Correlation of preoperative MRI and the pathologic examination. Pediatr Radiol 23: 421–424
3. Norton KI, Hermann G, Abdelwahab IF, et al (1991) Epiphyseal involvement in osteosarcoma. Radiology 180: 813–816
4. Onikul E, Fletcher BD, Parham DM, et al (1996) Accuracy of MR imaging for estimating intraosseous extent of osteosarcoma. AJR 167: 1211–1215
5. Reddick WE, Bhargava R, Taylor JS, et al (1995) Dynamic contrast-enhanced MR imaging of osteosarcoma response to neoadjuvant chemotherapy. J Magn Reson Imaging 5: 689–694
6. Van der Woude HJ, Bloem JL, Verstraete KL, et al (1995) Osteosarcoma and Ewing's sarcoma after neoadjuvant chemotherapy: value of dynamic MR imaging in detecting viable tumor before surgery. AJR 165: 593–598
7. Fletcher BD, Hanna SL, Fairclough DL, et al (1992) Pediatric musculoskeletal tumors: use of dynamic, contrast-enhanced MR imaging to monitor response to chemotherapy. Radiology 184: 243–248
8. Verstraete KL, De Deene Y, Roels H, et al (1994) Benign and malignant musculoskeletal lesions: dynamic contrast-enhanced MR imaging – parametric "first-pass" images depict tissue vascularization and perfusion. Radiology 192: 835–843
9. Iwasawa T, Tanaka Y, Aida N, et al (1997) Microscopic intraosseous extension of osteosarcoma: assessment on dynamic contrast-enhanced MRI. Skeletal Radiol 26: 214–221
10. Fletcher BD, Wall JE, Hanna SL (1993) Effect of hematopoietic growth factors on MR images of bone marrow in children undergoing chemotherapy. Radiology 189: 745–751
11. Ryan SP, Weinberger E, White KS, et al (1995) MR imaging of bone marrow in children with osteosarcoma: effect of granulocyte colony-stimulating factor. AJR 165: 915–920
12. Meyer WH, Pratt CB, Rao B, et al (1997) Curative therapy for osteosarcoma without cisplatin – preliminary results of SJCRH OS-91. Proc Annu Meet Am Soc Clin Oncol 16: 512 a
13. Reddick WE, Bhargava R, Taylor JS, et al (1995) Dynamic contrast-enhanced MR imaging evaluation of osteosarcoma response to neoadjuvant chemotherapy. J Magn Reson Imaging 5: 689–694
14. Reddick WE, Langston JW, Meyer WH, et al (1994) Discrete signal processing of dynamic contrast-enhanced MR imaging: statistical validation and preliminary clinical application. J Magn Reson Imaging 4: 397–404
15. Tofts PS (1997) Modeling tracer kinetics in dynamic Gd-DTPA MR imaging. J Magn Reson Imaging 7: 91–101
16. Brix G, Semmler W, Port R, et al (1991) Pharmacokinetic parameters in CNS Gd-DTPA enhanced MR imaging. J Comput Assist Tomogr 15: 621–628
17. Hoffmann U, Brix G, Knopp MV, et al (1995) Pharmacokinetic mapping of the breast: a new method for dynamic MR mammography. Magn Reson Med 33: 506–514
18. Weinmann H-J, Laniado M, Mutzel W (1984) Pharmacokinetics of GdDTPA/dimeglumine after intravenous injection into healthy volunteers. Physiol Chem Phys Med NMR 16: 167–172
19. Bloembergen N, Morgan LO (1961) Proton relaxation times in paramagnetic solutions. Effects of electron spin relaxation. J Chem Phys 34: 842–850
20. Luz Z, Meiboom S (1964) Proton relaxation in dilute solutions of cobalt (II) and nickel (II) ions in methanol and the rate of methanol exchange of the solvation sphere. J Chem Phys 40: 2686–2692
21. Zur Y, Stokar S, Bendel P (1988) An analysis of fast imaging sequences with steady-state transverse magnetization refocusing. Magn Reson Med 6: 175–193
22. Buxton RB, Edelman RR, Rosen BR, et al (1987) Contrast in rapid MR imaging: T1- and T2-weighted imaging. J Comput Assist Tomogr 11: 7–16
23. Dorfman DD, Alf E Jr (1969) Maximum likelihood estimation of parameters of signal detection theory and determination of confidence intervals – rating-method data. J Math Psychol 6: 487–496
24. Grey DR, Morgan BJT (1972) Some aspects of ROC curve-fitting: normal and logistic models. J Math Psychol 9: 128–139
25. Kumano M, Tamura K, Hamada T, et al (1983) Evaluation of bone diseases using dynamic bone scintigraphy. Nippon Acta Radiol 43: 1393–1406
26. Rao BN, Champion JE, Pratt CB, et al (1983) Limb salvage procedures for children with osteosarcoma: an alternative to amputation. J Pediatr Surg 18: 901–908
27. Pratt CB, Champion JE, Fleming ID, et al (1990) Adjuvant chemotherapy for osteosarcoma of the extremity. Long-term results of two consecutive prospective protocol studies. Cancer 65: 439–445